Title

The regulatory and transcriptional landscape associated with carbon utilization in a filamentous fungus

Journal

Proceedings of the National Academy of Sciences of the United States of America, 117(11)

ISSN

0027-8424

Authors

Wu, Vincent W

Thieme, Nils

Huberman, Lori B

et al.

Publication Date

2020-03-17

DOI

10.1073/pnas.1915611117

Peer reviewed

The regulatory and transcriptional landscape associated with carbon utilization in a filamentous fungus

Vincent W. Wu[a,b], Nils Thieme[c,1], Lori B. Huberman[a,b], Axel Dietschmann[c,2], David J. Kowbel[a], Juna Lee[d], Sara Calhoun[d], Vasanth R. Singan[d], Anna Lipzen[d], Yi Xiong[a,b,3], Remo Monti[d], Matthew J. Blow[d], Ronan C. O'Malley[d], Igor V. Grigoriev[a,d,e], J. Philipp Benz[c], and N. Louise Glass[a,b,e,4]

[a]Department of Plant and Microbial Biology, University of California, Berkeley, CA 94720; [b]Energy Biosciences Institute, University of California, Berkeley, CA 94704; [c]Holzforschung München, Technical University of Munich School of Life Sciences Weihenstephan, Technical University of Munich, 85354 Freising, Germany; [d]US Department of Energy Joint Genome Institute, Lawrence Berkeley National Laboratory, Berkeley, CA 94720; and [e]Environmental Genomics and Systems Biology, Lawrence Berkeley National Laboratory, Berkeley, CA 94720

Edited by Jay C. Dunlap, Geisel School of Medicine at Dartmouth, Hanover, NH, and approved January 20, 2020 (received for review September 10, 2019)

Filamentous fungi, such as *Neurospora crassa*, are very efficient in deconstructing plant biomass by the secretion of an arsenal of plant cell wall-degrading enzymes, by remodeling metabolism to accommodate production of secreted enzymes, and by enabling transport and intracellular utilization of plant biomass components. Although a number of enzymes and transcriptional regulators involved in plant biomass utilization have been identified, how filamentous fungi sense and integrate nutritional information encoded in the plant cell wall into a regulatory hierarchy for optimal utilization of complex carbon sources is not understood. Here, we performed transcriptional profiling of *N. crassa* on 40 different carbon sources, including plant biomass, to provide data on how fungi sense simple to complex carbohydrates. From these data, we identified regulatory factors in *N. crassa* and characterized one (PDR-2) associated with pectin utilization and one with pectin/hemicellulose utilization (ARA-1). Using in vitro DNA affinity purification sequencing (DAP-seq), we identified direct targets of transcription factors involved in regulating genes encoding plant cell wall-degrading enzymes. In particular, our data clarified the role of the transcription factor VIB-1 in the regulation of genes encoding plant cell wall-degrading enzymes and nutrient scavenging and revealed a major role of the carbon catabolite repressor CRE-1 in regulating the expression of major facilitator transporter genes. These data contribute to a more complete understanding of cross talk between transcription factors and their target genes, which are involved in regulating nutrient sensing and plant biomass utilization on a global level.

transcriptional networks | plant biomass deconstruction | nutrient sensing | DAP-seq | RNA-seq

In nature, fungi must integrate acquisition of nutrients with metabolism, growth, and reproduction. Fungal deconstruction of plant biomass requires the ability to efficiently produce and secrete large quantities of secreted plant cell wall-degrading enzymes (PCWDEs). Turnover of plant biomass by fungi is an ecosystem function (1), as well as an attribute that has been harnessed industrially to convert plant biomass to simple sugars and, in turn, high value compounds (2). The plant cell wall is composed of a complex and integrated set of polysaccharides that can vary across tissue type and plant species. Cellulose is the most recalcitrant and most abundant cell wall polysaccharide and is composed of β-1,4–linked D-glucose residues arranged in linear chains. Hemicelluloses represent about 20 to 35% of primary plant cell wall biomass and include polysaccharides with β-1,4–linked backbones, such as xylan, xyloglucan, and mannan. Pectin is a heterogeneous structure with an abundance of D-galacturonic acid, L-rhamnose, and L-arabinose. The two most common forms of pectin are homogalacturonan, which is composed of a D-galacturonic acid backbone, and rhamnogalacturonan I, which has a backbone consisting of alternating galacturonic acid and rhamnose residues. Both forms have a diverse array of side chains (3). Pectins are cross-linked with hemicellulose and cellulose and affect plant cell wall pore size, flexibility, and strength. Lignin, which adds rigidity to the plant cell wall, is composed of polymers of aromatic residues and is very recalcitrant to deconstruction (4).

Significance

Microorganisms have evolved signaling networks to identify and prioritize utilization of carbon sources. For fungi that degrade plant biomass, such as *Neurospora crassa*, signaling networks dictate the metabolic response to carbon sources present in plant cell walls, resulting in optimal utilization of nutrient sources. However, within a fungal colony, regulatory hierarchies associated with activation of transcription factors and temporal and spatial production of proteins for plant biomass utilization are unclear. Here, we perform expression profiling of *N. crassa* on simple sugars to complex carbohydrates to identify regulatory factors and direct targets of regulatory transcription factors using DNA affinity purification sequencing (DAP-seq). These findings will enable more precise tailoring of metabolic networks in filamentous fungi for the production of second-generation biofuels.

Author contributions: V.W.W., N.T., L.B.H., S.C., R.C.O., I.V.G., J.P.B., and N.L.G. designed research; V.W.W., N.T., L.B.H., A.D., D.J.K., J.L., S.C., V.R.S., A.L., Y.X., R.M., M.J.B., and R.C.O. performed research; V.W.W. contributed new reagents/analytic tools; V.W.W., N.T., L.B.H., A.D., D.J.K., S.C., Y.X., M.J.B., R.C.O., I.V.G., J.P.B., and N.L.G. analyzed data; and V.W.W., N.T., L.B.H., J.P.B., and N.L.G. wrote the paper.

The authors declare no competing interest.

This article is a PNAS Direct Submission.

Data deposition: The RNA-seq data reported in this paper have been deposited in the Joint Genome Institute (JGI) Genome Portal (https://genome.jgi.doe.gov/portal/TheFunENCproject/TheFunENCproject.info.html), in the National Center for Biotechnology Information (NCBI) Sequence Read Archive (accession no. SRP133337), and in the NCBI BioProject database (ID PRJNA594366). Data are also provided for processed RNA-seq experiments in Datasets S1, S4, S5, and S7. DAP-seq data reported in this paper have been deposited in the NCBI Sequence Read Archive (accession no. SRP133627). Data are also provided for processed DAP-seq experiments in Dataset S5.

[1]Present address: Microbiology, Technical University of Munich School of Life Sciences Weihenstephan, Technical University of Munich, 85354 Freising, Germany.

[2]Present address: Department of Infection Biology, University Hospital Erlangen and Friedrich-Alexander University, Erlangen-Nürnberg, 91054 Erlangen, Germany.

[3]Present address: Amyris, Inc., Emeryville, CA 94608.

[4]To whom correspondence may be addressed. Email: lglass@berkeley.edu.

This article contains supporting information online at https://www.pnas.org/lookup/suppl/doi:10.1073/pnas.1915611117/-/DCSupplemental.

First published February 28, 2020.

Although biochemical activities of select PCWDEs have been investigated in a variety of filamentous fungi, how fungi sense complex carbohydrates in plant biomass and how that sensing is transduced intracellularly into a hierarchical metabolic response resulting in optimal production of PCWDEs and integration of cellular metabolism are unclear. The production of PCWDEs is dependent on transcription factors that modulate expression of these genes upon appropriate nutrient sensing. In *Neurospora crassa*, *Aspergillus nidulans*, *Aspergillus oryzae*, and *Penicillium oxalicum*, the transcription factor CLR-2 (ClrB/ManR) is the major regulator of genes involved in the deconstruction of cellulose (5, 6), while in *Trichoderma reesei* and *Aspergillus niger*, the transcription factor Xyr1/XlnR regulates genes involved in both cellulose and hemicellulose degradation (7, 8). In species like *N. crassa* and *Fusarium graminearum*, XlnR homologs regulate genes involved in hemicellulose utilization (9, 10). Transcription factors associated with pectin deconstruction include RhaR/PDR-1 and GaaR. In *A. niger* and *N. crassa*, RhaR/PDR-1 is required for rhamnose utilization (11, 12), while in *Botrytis cinerea* and *A. niger*, GaaR is responsible for galacturonic acid utilization (13, 14). In *A. niger*, the AraR transcription factor modulates arabinose utilization, while a different transcription factor (Ara1) functions in an analogous manner in *Magnaporthe oryzae* and *T. reesei* (15, 16). Additional transcriptional regulators that affect expression of genes encoding PCWDEs include the carbon catabolite repressor protein CreA/CRE-1 (17, 18), COL-26/BglR (19, 20), and VIB-1/Vib1 (21, 22).

Here, we performed transcriptional profiling of *N. crassa* on 40 different carbon sources to provide data on how fungi sense simple to complex carbohydrates and analyzed profiling data to identify regulatory factors associated with carbon source sensing and the regulation of transcriptional responses. From this approach, two transcription factors, one involved in pectin utilization, PDR-2, and one involved in pectin and hemicellulose utilization, ARA-1, were identified and their regulons characterized. Using in vitro DNA affinity purification sequencing (DAP-seq) of transcription factors involved in regulating PCWDE-encoding genes led to a more complete understanding of the direct targets of transcription factors that regulate PCWDE gene expression and of the cross talk between transcription factors involved in regulating nutrient sensing on a global level. In particular, our data clarified the role of VIB-1 in the regulation of genes encoding PCDWEs and nutrient scavenging and identified a previously overlooked mechanism of the carbon catabolite repressor protein CreA/CRE-1 in regulating cellular responses to carbon sources.

Results

***N. crassa* Carbon Metabolism Is Distinctly Regulated in Response to Different Carbon Sources.** To improve our understanding of how regulatory networks are integrated during plant biomass utilization by filamentous fungi, we assessed gene expression patterns across 40 different carbon conditions in *N. crassa* (*SI Appendix*, Table S1). To reduce the effects of differential growth on gene expression in different carbon sources, we performed switch experiments where wild-type (WT) *N. crassa* cells (FGSC2489) were pregrown in sucrose as the sole carbon source (16 h), washed, and then transferred to media containing the experimental carbon source for 4 h prior to RNA extraction. The carbon sources were divided into three categories: plant biomass, complex polysaccharides found in the plant cell wall, and the monosaccharide and disaccharide building blocks that make up these complex polysaccharides. We compiled a list of 113 genes encoding predicted PCWDEs in the *N. crassa* genome (*SI Appendix*, Table S2) and assessed expression of this gene set across our carbon panel (Fig. 1*A* and Dataset S1).

At low concentrations, various monosaccharides, disaccharides, and oligosaccharides induce the expression of genes encoding PCWDEs (23, 24). We exposed *N. crassa* to 19 different monosaccharides and disaccharides at 2 mM concentration; this concentration of cellobiose was previously shown to induce robust expression of cellulolytic genes in *N. crassa* (23) (*SI Appendix*, Table S1). As predicted, *N. crassa* induced genes encoding cellulases in response to cellobiose, genes encoding starch-degrading enzymes in response to maltose, genes encoding hemicellulases in response to xylose and arabinose, and genes encoding pectin deconstruction enzymes upon exposure to rhamnose and galacturonic acid (Fig. 1*A* and Dataset S1). However, individual sugars were also capable of inducing expression of PCWDEs not responsible for degrading their parent polymer. For example, cellobiose induced expression of some genes encoding some xylanases and pectinases in addition to cellulases, and arabinose induced expression of some genes encoding some cellulases in addition to arabinases (Dataset S1). These data indicate metabolic cross talk between sugar-sensing pathways and/or overlap in regulatory networks. *N. crassa* also showed strong transcriptional responses to complex plant biomass substrates, such as corn stover (a monocotyledonous plant of the grass family) and wingnut (*Pterocarya*; a hardwood tree from the walnut family) (Fig. 1*A*).

Monosaccharides, disaccharides, and oligosaccharides require transport into the cell for utilization and/or signaling for induction of genes encoding PCWDEs. Annotated sugar transporters belong to the major facilitator superfamily (MFS) and led us to hypothesize that uncharacterized sugar transporters would also come from this protein family. To test this hypothesis, we constructed a maximum-likelihood tree using protein sequences from all MFS transporters in the *N. crassa* genome (*SI Appendix*, Fig. S1). The majority of predicted sugar transporters, with the exception of NCU05897 (fucose permease) and NCU12154 (maltose permease), fell into a single monophyletic clade corresponding to family 2.A.1.1 of the Transporter Classification Database (25). Of the predicted sugar transporters in this clade, five unannotated MFS transporters (NCU04537, NCU05350, NCU05585, NCU06384, and NCU07607) had increased expression on unique sugars and complex carbon sources, suggesting potential involvement in catabolism of those carbon sources (*SI Appendix*, Fig. S1 and Dataset S1).

To evaluate cross talk between regulatory pathways that coordinate expression of PCWDEs, we performed weighted gene coexpression network analysis (WGCNA) (26) across the transcriptional dataset and identified 28 modules of coexpressed genes (Fig. 1*B* and Dataset S2) that showed enrichment of specific functional classifications (*SI Appendix*, Fig. S2). The majority of PCWDE genes were found within three modules. Module 1 (red; $n = 153$) contained genes encoding PCWDEs that are up-regulated in response to cellulose and hemicellulose along with notable transcription factors *xlr-1*, *clr-1*, *clr-2*, *hac-1*, and *vib-1* (21, 27, 28). This module also contained 55 genes that encoded hypothetical proteins. Module 2 (yellow; $n = 42$) contained the majority of predicted pectin metabolic genes (28) and eight genes encoding hypothetical proteins. Module 3 (blue; $n = 42$) contained a number of predicted pentose catabolic genes along with some notable xylanases and xylose transporters and nine genes encoding hypothetical proteins (Dataset S2 and *SI Appendix*, Fig. S2). An additional module (module 4; $n = 142$; midnight blue) clustered closely with modules 1 and 3. This module was significantly enriched for genes encoding endoplasmic reticulum (ER) and protein-processing proteins (cellular transport and protein fate; *SI Appendix*, Fig. S2) that are coregulated with genes encoding cellulases and xylanases, such as various COPII proteins, SEC-61, and KEX2 (Datasets S1 and S2). This module also included genes encoding 29 hypothetical proteins.

Defining the PCWDE Transcriptional Network. Prior studies in *N. crassa* identified conserved transcription factors that are positive regulators of cellulase and some hemicellulase genes (CLR-1/CLR-2), xylanase and xylose utilization genes (XLR-1), pectin-degrading genes (PDR-1), and starch catabolic genes (COL-26)

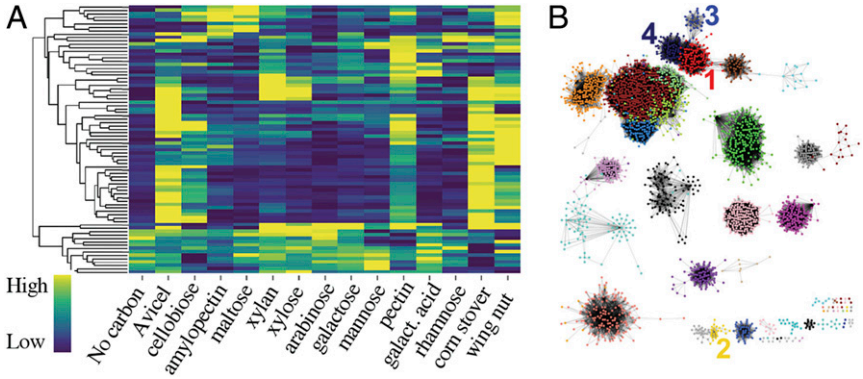

Fig. 1. Hierarchical clustering and WGCNA of *N. crassa* transcriptome across carbon sources. (*A*) Hierarchical clustering of the normalized counts (FPKMs) of genes encoding PCWDEs in cells shifted to the indicated carbon sources. All disaccharides and monosaccharides are at 2 mM concentration, and complex carbohydrates are at 1% (wt/vol). The color bar represents the spectrum from lowest normalized count to highest normalized count for each gene centered on mean expression; each gene has a different range of FPKMs. (*B*) Coexpression network with nodes representing genes colored by modules and edges between genes with correlated expression profiles, shown using Cytoscape (79) (Dataset S2). Four modules enriched in genes encoding PCWDEs and polysaccharide metabolism are labeled. Module 1 (red): genes associated cellulose and hemicellulose utilization. Module 2 (yellow): genes associated with pectin deconstruction. Module 3 (blue): pentose catabolic and xylan utilization genes. Module 4 (midnight blue): genes encoding ER- and protein-processing proteins (Dataset S2). Total number of genes shown in the network is 3,282.

(10, 11, 19, 27). We hypothesized that it would be possible to identify additional regulators involved in plant cell wall degradation by looking for transcription factors with a similar expression profile to a specific class of genes encoding PCWDEs using hierarchical clustering. A systematic analysis of expression profiles of 336 proteins with predicted DNA-binding domains identified 34 additional transcription factors that were specifically induced on different plant biomass components (Dataset S3). We hypothesized that strains carrying a deletion of a transcription factor would display an altered transcriptional profile under the conditions where they were most highly expressed (Dataset S3). When the corresponding deletion strains were tested under the respective induction conditions, a majority of the 34 transcription factor deletion mutants did not display a clear expression phenotype compared to the parental strain, FGSC2489. However, deletion mutants for two transcription factors showed a consistent and obvious role in PCWDE expression, NCU04295 and NCU05414 (Dataset S4).

The expression of NCU04295 clustered with genes encoding pectin-degrading enzymes (Dataset S4) and a ΔNCU04295 mutant showed decreased expression levels of genes necessary for pectin utilization when grown in presence of pectin-rich citrus peel compared to WT cells on citrus peel (Fig. 2 *A* and *B* and Dataset S4). The genes with the largest decrease in expression level in ΔNCU04295 compared to WT included pectate lyases genes *ply-1* and *ply-2* (NCU06326 and NCU08176), the galacturonic acid transporter gene *gat-1* (NCU00988), the exo-polygalacturonase gene *gh28-2* (NCU06961), and orthologs of *gaaA*, *gaaB*, and *gaaC* (NCU09533, NCU07064, and NCU09532, respectively), encoding enzymes for galacturonic acid catabolism (Fig. 2*B* and Dataset S4). The predicted protein sequence of NCU04295 showed similarity (~50% amino acid identity) to GaaR, which plays a role in galacturonic acid metabolism in *B. cinerea* and *A. niger* (13, 14). We therefore named NCU04295 *pdr-2* for pectin degradation regulator-2. Consistent with its predicted function, the Δ*pdr-2* mutant showed a severe growth defect in medium containing pectin or galacturonic acid as the sole carbon source and significantly reduced pectate lyase and endo-polygalacturonanase activity (Fig. 2 *C* and *D*). A second pectin degradation regulator previously identified in *N. crassa*, *pdr-1*, also shows a severe growth defect on pectin (11). However, unlike Δ*pdr-1* cells, Δ*pdr-2* cells grew on L-rhamnose as the sole carbon source (*SI Appendix*, Fig. S3), suggesting distinct roles for PDR-2 and PDR-1 in regulating pectin degradation. A strain bearing both *pdr-1* and *pdr-2* deletions mimicked the phenotype of either a Δ*pdr-1* or a Δ*pdr-2* mutant (Fig. 2 *C* and *D*), but did not cause a complete abolition of growth with pectin as the sole carbon source (*SI Appendix*, Fig. S3).

NCU05414 displayed high expression on *Miscanthus* biomass (Dataset S1). When compared to WT cells exposed to 1% *Miscanthus*, a ΔNCU05414 mutant showed reduced expression of genes encoding several arabinosidases (NCU09924, NCU9775), two β-xylosidases (NCU00709, NCU09923), the L-arabinose transporter *lat-1* (NCU02188), and L-arabinitol dehydrogenase *ard-1* (NCU00643) (Fig. 2*E* and Dataset S4), suggesting that the ΔNCU05414 mutant would be defective for utilization of arabinan, arabinose, and galactose. As predicted, the ΔNCU05414 strain showed dramatically reduced growth on 2% arabinan, arabinose, and galactose, but was able to metabolize hemicellulose and pectin substrates (Fig. 2*F*). When NCU05414 was placed under the regulation of the strong constitutive promoter *gpd-1* (oxNCU05414), cells showed increased growth on arabinose relative to WT (*SI Appendix*, Fig. S3) and increased expression of *ard-1* (Fig. 2*G*), further supporting positive regulation of arabinose metabolic genes by NCU05414. The NCU05414 predicted protein showed significant similarity to the Ara1 protein in *T. reesei* and *Magnaporthe oryzae*, where it plays a role in arabinose metabolism and arabinose and galactose catabolism, respectively (16, 29). We therefore named NCU05414 *ara-1*.

Many PCWDEs involved in degradation of heterogeneous substrates like pectin and hemicellulose are under the control of multiple transcription factors. We constructed regulons of transcription factors CLR-1, CLR-2, XLR-1, PDR-1, PDR-2, and ARA-1 that are important for plant biomass deconstruction by identifying genes encoding PCWDE that were down-regulated by at least $2^{1.5}$ (2.8)-fold between Δ*clr-1*, Δ*clr-2*, Δ*xlr-1*, Δ*pdr-2*, and Δ*ara-1* mutants versus WT cells (Dataset S4); genes up-regulated in these mutants were similar to genes up-regulated during the starvation response, which indicated these transcription factors function positively. We also included data obtained under identical conditions as performed here from our previous studies for COL-26 and PDR-1 (11, 19). The regulons of CLR-1, CLR-2, XLR-1, PDR-1, PDR-2, ARA-1, and COL-26 showed extensive overlap (Fig. 3). As an example, the expression of the putative acetylxylan esterase gene (*ce1-1* NCU04870), an enzyme responsible for cleaving acetyl groups from xylan and critically important for increasing accessibility of xylan to xylanases, showed a 20-fold decrease in expression levels in Δ*clr-2* cells

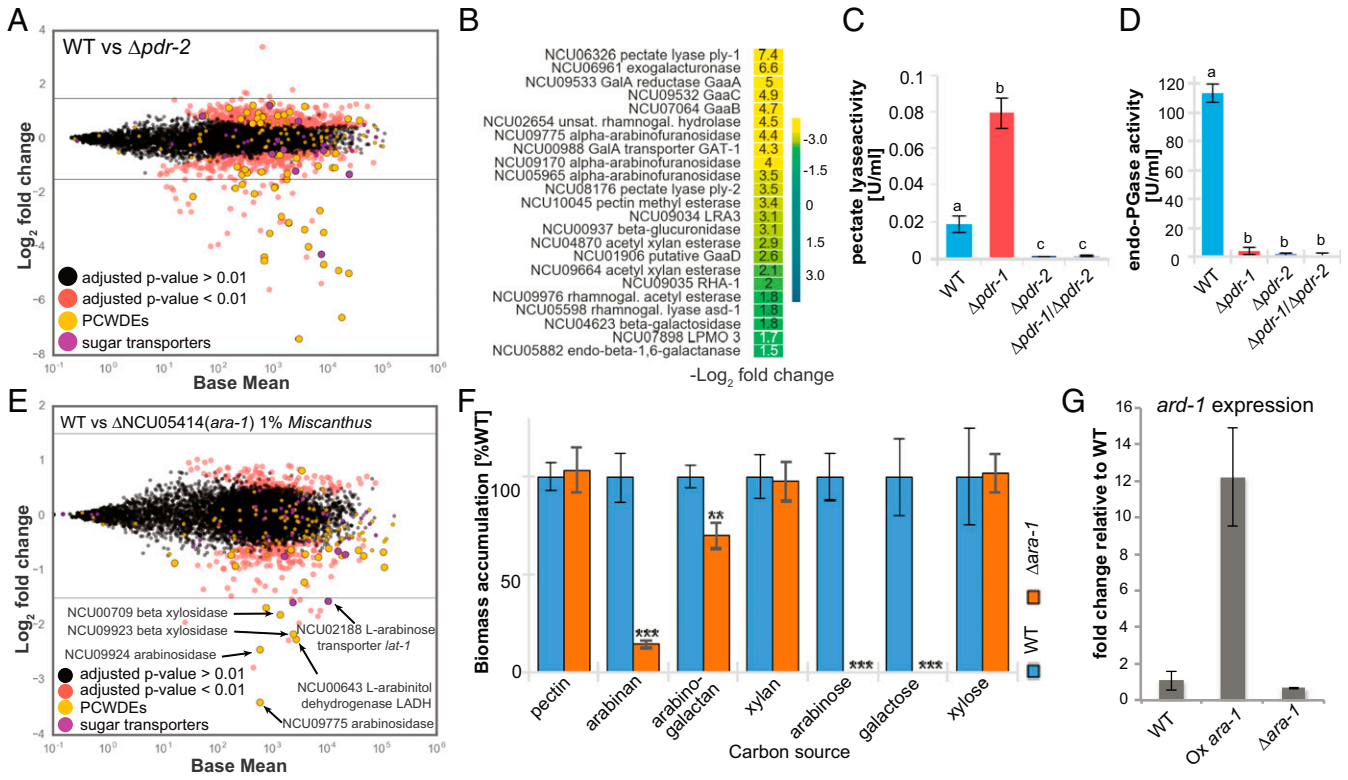

Fig. 2. The transcription factor *pdr-2* regulates pectin degradation, and the transcription factor *ara-1* regulates arabinose utilization. (*A*) Differential expression analysis of ΔNCU04295 (*pdr-2*) relative to WT cells after a shift to 1% (wt/vol) citrus peel (Dataset S1). PCWDEs are yellow, and sugar transporters are purple. "Base mean" is the mean of normalized counts for triplicates of both conditions tested. (*B*) Differential expression of PCWDEs ranked by degree of $\log_2$ fold change from *A*. (*C*) Pectate lyase and (*D*) endo-polygalacturonanase (endo-PGase) activities of Δ*pdr-1*, Δ*pdr-2*, and Δ*pdr-1* Δ*pdr-2* mutants relative to WT. Significance was determined by ANOVA followed by a post hoc Tukey's test. The letters above each bar indicate statistical significance with a mean difference of $P < 0.05$. (*E*) Differential expression analysis of ΔNCU05414 (*ara-1*) in comparison to WT after cultures were shifted to 1% (wt/vol) Miscanthus (Dataset S1). PCWDEs are in yellow, and sugar transporters are in purple. Base mean is the mean of normalized counts for triplicates of both conditions tested. (*F*) Relative biomass accumulation of Δ*ara-1* normalized to WT cultured in the indicated carbon sources. Significance was determined by an independent two-sample *t* test of WT against Δ*ara-1* with $^{**}P < 0.01$ and $^{***}P < 0.001$ ($n = 3$). (*G*) Relative *ard-1* (L-arabinitol dehydrogenase [LADH]) expression relative to *act* after shift to arabinose in Δ*ara-1* and in an *ara-1* overexpression strain (Ox *ara-1*). For *C*, *D*, *F*, and *G*, error bars represent SD ($n \geq 3$).

after a shift to Avicel, a 500-fold decrease in expression in Δ*xlr-1* cells after a shift to xylan, and a 7-fold decrease in expression in Δ*pdr-2* cells after a shift to citrus peel relative to WT cells (Dataset S4). Moreover, the *ce1-1* promoter was shown to be directly bound by both XLR-1 and CLR-2 by chromatin immunoprecipitation sequencing (ChIP-seq) (10).

Utilizing DAP-Seq to Identify Direct Targets of *N. crassa* Transcription Factors. The transcriptional regulons associated with plant biomass deconstruction identified above could be due to direct or indirect regulation of target genes by a particular transcription factor. To define the direct regulons of transcription factors involved in plant biomass deconstruction, we used DAP-seq, where in vitro-synthesized transcription factors are used for affinity purification of bound oligonucleotides in sheared genomic DNA, which are subsequently identified via DNA sequence analyses (30). To ensure that DAP-seq was an effective method for identifying direct binding sites of transcription factors involved in plant cell wall deconstruction in *N. crassa*, we confirmed the DNA binding sites of CLR-1 and XLR-1, for which ChIP-seq data are available (10).

We reanalyzed promoter regions of genes (defined as within 3 kb of the ATG start site) bound by XLR-1 identified via ChIP-seq (10) (Dataset S5) and bound promoter regions identified via DAP-seq where transcription was reduced by at least $2^{1.5}$ (2.8)-fold via differential RNA-seq analysis of WT versus an Δ*xlr-1* mutant (Datasets S4 and S5). We identified 85 XLR-1 target genes using ChIP-seq data and 78 genes via DAP-seq, with 47 genes shared between the two datasets (*SI Appendix*, Fig. S4 *A*, *C*, and *F* and Dataset S5). The binding site sequences from the 78 genes identified in the DAP-seq dataset were used to build an XLR-1 consensus binding motif, which was comparable to the one reported from ChIP-seq data analysis (10) (*SI Appendix*, Fig. S4*G*). Using the same methods to explore CLR-2, we identified 87 genes with CLR-2–bound promoters via DAP-seq and 65 genes with CLR-2–bound promoters via ChIP-seq; 48 genes were shared between datasets (*SI Appendix*, Fig. S4 *D*–*F* and Datasets S4 and S5). Slight differences were identified in the CLR-2 consensus binding sequence using DAP-seq versus that previously reported for ChIP-seq data (10) (*SI Appendix*, Fig. S4*G*).

Neither the ChIP-seq nor DAP-seq method reliably identified genes differentially expressed between WT and the transcription factor mutant under the conditions tested. For example, ChIP-seq performed on CLR-2 identified 158 genes with promoter regions bound, while DAP-seq identified 1,683; however, only 87 of the DAP-seq bound genes were differentially expressed in a Δ*clr-2* mutant relative to WT cells. For XLR-1, ChIP-seq identified 1,117 genes, while DAP-seq identified 531; 78 of these genes were differentially expressed in a Δ*xlr-1* mutant relative to WT cells (Dataset S5). We assessed the relationship between DAP-seq peak intensity, expression values, and distance to translation start site in data for XLR-1 and CLR-2 target genes identified by DAP-seq/RNA-seq analyses (*SI Appendix*, Fig. S5). A trend toward DAP-seq peaks in/near the predicted promoter region of

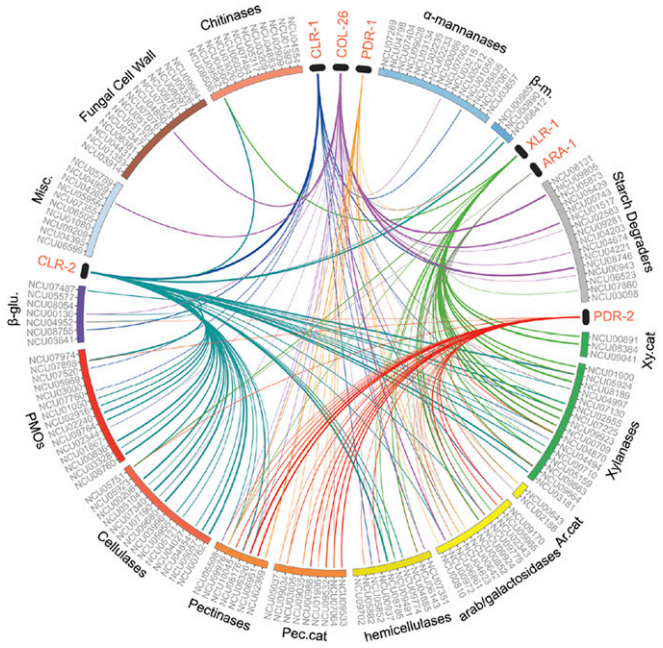

Fig. 3. Overlapping regulons of major PCWDE regulators in *N. crassa*. Plot built with Circos, version 0.69 (80), to display positive regulation of catabolic CAZymes by indicated transcription factors (red) derived from the identification of genes that showed differential expression of $2^{1.5}$-fold between WT and transcription factor mutant (Dataset S1). CAZymes are divided into functional groups displayed on the outer edge of the plot. Ar, arabinose; Ar. cat., arabinose catabolism; β-glu, β-glucosidases; β-m, β-mannanases; Pec. cat, pectin catabolism; PMO, polysaccharide monooxygenases; Xy, xylose. Each CAZyme is represented by its gene ID. Each line represents genes with significantly different expression between WT and a transcription factor deletion mutant under the following conditions: Δ*clr-1* and Δ*clr-2* shifted to 1% Avicel, Δ*col-26* shifted to 2 mM maltose (19), Δ*pdr-1* shifted to 1% pectin (11), Δ*pdr-2* shifted to 1% citrus peel, Δ*ara-1* shifted to 1% *Miscanthus*, and Δ*xlr-1* shifted to 1% xylan (Dataset S4). The thickness of the line corresponds to degree of fold change in the transcription factor deletion mutants compared to WT cells (11, 19), with thicker lines indicating a higher fold change.

genes (within ∼1 kbp from the translational start site) and a correlation with being positively regulated by XLR-1 and CLR-2 was identified. Comparisons of differential expression analyses between WT and transcription factor mutants helped to filter the ChIP-seq and DAP-seq datasets for biologically relevant genes for these specific transcription factors. For the remaining genes whose expression was not altered in the transcription factor mutants, it is unclear whether they are "false positive" or genes that might be regulated by CLR-2 or XLR-1 under conditions that were not assessed in this study.

In *T. reesei,* a constitutively active *xyr1* allele (ortholog to *N. crassa xlr-1*) contains a single amino acid substitution (alanine to valine) in the C-terminal predicted α-helix (31). The construction of the orthologous mutation (A828V) in *N. crassa xlr-1* results in a strain that shows inducer-independent expression and production of hemicellulases (10). To test whether this mutation affected the binding affinity of XLR-1, we also performed DAP-seq on the XLR-1^{A828V} mutant. The binding targets of the XLR-1^{A828V} mutant largely overlapped with the binding targets of XLR-1, indicating that the A828V mutation has little or no influence on XLR-1 DNA binding affinity (*SI Appendix*, Fig. S4 *B* and *F* and Dataset S5).

DAP-Seq Suggests a Multitiered System of CRE-1–Mediated Carbon Catabolite Repression. CRE-1 is a major regulator of carbon catabolite repression, a process through which the expression of genes involved in the utilization of nonpreferred carbon sources is repressed in the presence of preferred carbon sources (32). Although many PCWDEs are known to be regulated by carbon catabolite repression, it was unclear whether this repression was directly or indirectly mediated by CRE-1. Using DAP-seq, we identified 329 CRE-1 binding sites in 318 promoter regions, with 11 promoters showing two peaks (Dataset S5). The 318 genes with promoters bound by CRE-1 were enriched for 30 functional categories ($P < 1 \times 10^{-5}$) involved in metabolic activities (Dataset S6). The top 17 functional categories were all involved in carbon metabolism, specifically cellulose, hemicellulose, pectin, and starch catabolism, representing ∼50% of the total CRE-1 peaks and consistent with functions associated with CRE-1. We used the sequences from CRE-1–bound peaks to build a consensus core motif with the best-fit core motif being 5′-TSYGGGG-3′ ($E = 2.7 \times 10^{-23}$), similar to the 5′-SYGGRG-3′ motif described for CreA in *A. nidulans* (33) (*SI Appendix*, Fig. S3*C*).

If CRE-1 directly represses genes encoding PCWDEs, we would expect to see CRE-1 binding of PCWDE promoter regions. However, only 19 of 113 PCWDE genes had CRE-1 binding sites in the promoter (Dataset S5). According to the "double-lock" mechanism proposed for Cre1 in *Aspergillus nidulans* (34), indirect repression of PCWDE expression by CRE-1 could be due to either CRE-1 repression of transcription factors required for PCWDE gene activation or CRE-1 repression of genes necessary to activate those transcription factors. In our DAP-seq dataset, promoters for only two carbon transcription factors were bound by CRE-1, *clr-1* and *ara-1*. However, CRE-1 binding was highly biased for promoters of genes encoding MFS transporters (22 MFS genes), with 15 falling within the major sugar transporter clade (*SI Appendix*, Fig. S1), including one high-affinity glucose transporter, *hgt-1* NCU10021 (35) and additional uncharacterized transporters (NCU00809, NCU06522, NCU09287, NCU04537, NCU01494, NCU06384, and NCU05897).

An uncharacterized sugar transporter bound by CRE-1, *sut-28* (NCU05897; annotated as a fucose permease; *SI Appendix*, Fig. S1), is a predicted ortholog of the *A. niger* L-rhamnose transporter RhtA (36). The *sut-28* mutant showed reduced growth on L-rhamnose and, to a lesser extent, poly-galacturonic acid (Fig. 4*A*), and uptake of L-rhamnose in the Δ*sut-28* cells was eliminated (Fig. 4*B*). Similar to a Δ*pdr-1* mutant, Δ*sut-28* cells failed to activate expression of the rhamnose catabolic gene L-rhamnonate dehydratase (NCU09034) (Fig. 4*C*). The expression of *sut-28* was higher in Δ*cre-1* cells compared to WT when exposed to L-rhamnose or L-rhamnose and glucose (*SI Appendix*, Fig. S3*D*) and Δ*cre-1* cells showed increased L-rhamnose uptake compared to WT when exposed to pectin and glucose (Fig. 4*D*). These data supported the CRE-1 DAP-seq data indicating that CRE-1 negatively regulates the expression of *sut-28.*

CRE-1 also bound to the promoters of the cellodextrin transporters *cdt-1* (NCU00801), *cdt-2* (NCU08114), and *sut-12*/*cbt-1* (NCU05853) (37–40). Cells lacking both *cdt-1* and *cdt-2* are unable to activate cellulolytic gene transcription and do not grow on cellulose (41). The binding of CRE-1 to the promoter of *clr-1* likely contributes to the repression of cellulolytic genes by CRE-1, as CLR-1 positively regulates *clr-2*, the major regulator of cellulolytic genes in *N. crassa* (10, 27) (Dataset S5). Thus, our data suggested that cellulolytic gene expression is repressed by CRE-1 through a combination of direct binding to cellodextrin transporters, the transcription factor *clr-1*, and a few cellulolytic PCWDEs (Fig. 5).

For genes involved in hemicellulose deconstruction, CRE-1 binding sites were detected in the promoters of the arabinose-transporter *lat-1* (NCU02188) (28), xylose transporters NCU00821 and NCU04527 (42), the xylodextrin transporter *cdt-2*, which is required for WT levels of growth on xylan (39), and pentose transporters *xat-1* (NCU01132) and *xyt-1* (NCU05627) (43) (Fig. 5). CRE-1 binding peaks were not detected in the promoter of the

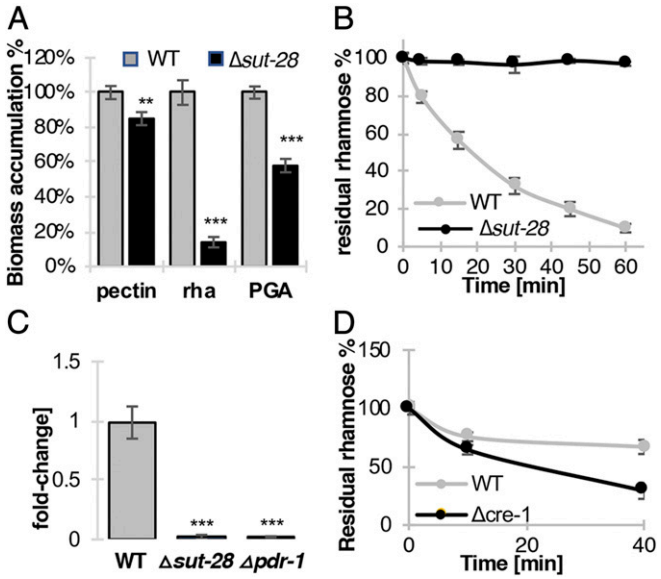

Fig. 4. *sut-28* expression and rhamnose transport activity in WT and Δ*cre-1* strains. (*A*) Relative biomass of FGSC2489 (WT) and Δ*sut-28* strains incubated in pectin, rhamnose, and polygalacturonic acid (PGA) as determined by dry weight. (*B*) Rhamnose uptake in FGSC2489 and Δ*sut-28* strains after induction on pectin. (*C*) Relative expression of NCU09034 (L-rhamnonate dehydratase) relative to *actin* (NCU04173) in FGSC2489 (WT), Δ*sut-28*, and Δ*pdr-1* strains after induction on rhamnose. (*D*) Rhamnose uptake in FGSC2489 and Δ*cre-1* strains induced with pectin plus glucose. Error bars represent SD ($n \geq 3$). Significance was determined by an independent two-sample *t* test of WT against Δ*sut-28* or Δ*pdr-1* mutants; $^{**}P < 0.01$ and $^{***}P < 0.001$.

major transcriptional regulator of xylan utilization, *xlr-1*, although CRE-1 binding sites were detected in the promoter of the arabinose utilization regulator, *ara-1*; an Δ*ara-1* mutant showed dramatically reduced growth on arabinan, arabinose, and galactose (Fig. 2). CRE-1 also directly bound to promoters of genes encoding xylanases, galactosidases, and arabinanases, as well as genes necessary for arabinose metabolism (Dataset S5 and Fig. 5).

CRE-1 was not bound to the *pdr-1* or *pdr-2* promoters, which are responsible for regulating the majority of pectinase genes in *N. crassa* (ref. 12 and Fig. 2*A*). However, CRE-1 binding sites were identified in the promoter of a major exo-polygalacturonase (NCU06961; *gh28-2*) as well as predicted metabolic enzymes for galacturonic acid utilization (*gaaA* ortholog NCU09533, *gaaB* ortholog NCU07064, and *gaaC* ortholog NCU09532) (Fig. 5 and Dataset S5).

Previous microarray data of a Δ*cre-1* mutant relative to WT under minimal medium conditions with sucrose as the sole carbon source showed that 75 genes showed increased expression levels (greater than twofold) in the Δ*cre-1* mutant (17), including seven genes encoding predicted MFS transporters (Dataset S5). Of these 75 genes, the promoters of 21 of them were bound by CRE-1 in the DAP-seq dataset (Dataset S5), a significant enrichment over expected value if random (3.5 genes). All seven of the predicted MFS transporters that showed increased expression in the Δ*cre-1* mutant relative to WT were bound by CRE-1. These MFS sugar transporters included NCU04537 (monosaccharide transporter), NCU04963 (high-affinity glucose transporter), NCU06026 (quinate permease), NCU05897 (*sut-28*), NCU10021 (*hgt-1*), NCU00821 (sugar transporter), and NCU05627 (high-affinity glucose transporter *ght-1*). The remaining set of 21 genes included a number of carbon metabolic enzymes and 5 genes encoding proteins of unknown function (Dataset S5). Thus, an important component of CRE-1 function includes the repression of genes encoding transporters that play a role in the uptake of signaling molecules that act as inducers of transcription factors and genes associated with cellulose, hemicellulose, and pectin utilization (Fig. 5).

DAP-Seq of VIB-1 Reveals a Global Role in Regulating Carbon Metabolism. VIB-1 is a Zn_2Cys_6 transcription factor first identified for its role in mediating self/nonself recognition and heterokaryon incompatibility in *N. crassa* (44, 45). The Δ*vib-1* mutant also shows severely reduced growth on Avicel and a weak induction of *clr-2* (21), a phenotype also observed in *T. reesei* Δ*vib1* strains (22). In addition to Avicel, the Δ*vib-1* mutant also had a severe growth defect on pectin and a moderate growth defect on xylan (*SI Appendix*, Fig. S6*A*).

RNA-seq was previously performed on Δ*vib-1* cells exposed to Avicel and carbon starvation conditions (21). Here, we performed additional RNA-seq experiments on the Δ*vib*-1 mutant exposed to 1% pectin or 1% xylan as the sole carbon source, 1% BSA as the sole carbon and nitrogen source, and 1% ground *Miscanthus* as the complete nutrient source (Dataset S7). RNA-seq data reflected the severity of growth phenotypes, as exposure to Avicel, pectin, and BSA displayed the greatest number of differentially expressed genes between WT and the Δ*vib-1* mutant. Consistent with its phenotype, the Δ*vib-1* mutant has a more similar expression profile to WT cells under xylan conditions.

Using DAP-seq, we identified VIB-1 binding sites within 1.5 kb upstream of the ATG start site of 1,742 genes (Dataset S5). The RNA-seq datasets were utilized to filter the DAP-seq data by limiting the set to genes with at least a $2^{1.5}$ (2.8)-fold change in gene expression in any of our six conditions. In total, we identified 238 direct target genes of VIB-1 (Dataset S7). Hierarchical clustering of gene expression data of these direct targets showed that one cluster included the majority of genes that were down-regulated in the Δ*vib-1* mutant in more than three conditions. We considered these genes to be the core regulon of VIB-1 (Fig. 6*A*). A consensus binding motif from VIB-1 peaks within the 1.5-kb promoter regions of core regulon genes showed conservation of three critical bases: T, A, and C (Fig. 6*B*).

The 56 gene VIB-1 core regulon included genes involved in heterokaryon incompatibility (*tol*, *pin-c*, and *het-6*) and a number of uncharacterized genes encoding proteins with predicted roles in heterokaryon incompatibility (HET domain proteins and genes with polymorphic alleles in wild populations; NCU03533, NCU05840, NCU07335, and NCU04453) (Dataset S7) (46). Most of the other annotated genes in the VIB-1 core regulon were associated with metabolism, including three arabinofuranosidases (NCU09170 NCU09975 and NCU02343), a β-xylosidase (NCU09923), three cellulose polysaccharide monooxygenases (NCU02240, NCU09764, and NCU02344), a starch active polysaccharide monooxygenase (NCU08746), a galacturonic acid transporter (*gat-1*; NCU00988), an exogalacturonase (NCU06961), rhamnogalacturonan acetylesterase (NCU09976), a secreted phospholipase (NCU06650), and acid phosphatase (*pho-3*; NCU08643) (Dataset S7) (Fig. 6*C*). Three genes encoding LaeA-like methyltransferase domains (NCU05841, NCU05832, and NCU05501) were in the core VIB-1 regulon and four additional LaeA-like genes were direct targets of VIB-1 (NCU04909, NCU04717, NCU04707, and NCU01148) (Dataset S7). LaeA is a regulator of secondary metabolism in ascomycete fungi first described in *A. nidulans* (47).

The *clr-2* and *pdr-2* genes were the only ones encoding transcription factors that were direct targets of VIB-1 (Fig. 6*C*). In the Δ*vib-1* mutant, expression of *clr-2* was reduced 5.2-fold relative to WT during exposure to Avicel, and expression of *pdr-2* was reduced 3.4-fold relative to WT during exposure to pectin. In addition to *clr-2* and *pdr-2*, a number of PCWDE-encoding genes were bound and regulated by VIB-1, including genes encoding enzymes in the core VIB-1 regulon (above), cellulases (*gh6-3*, NCU07190; *gh45-1*, NCU05121, NCU05751), arabinosidase (NCU05965), rhamnogalacturonase (NCU05598), rhamnogalacturonan acetylesterase (NCU09976), a pectinesterase (NCU10045),

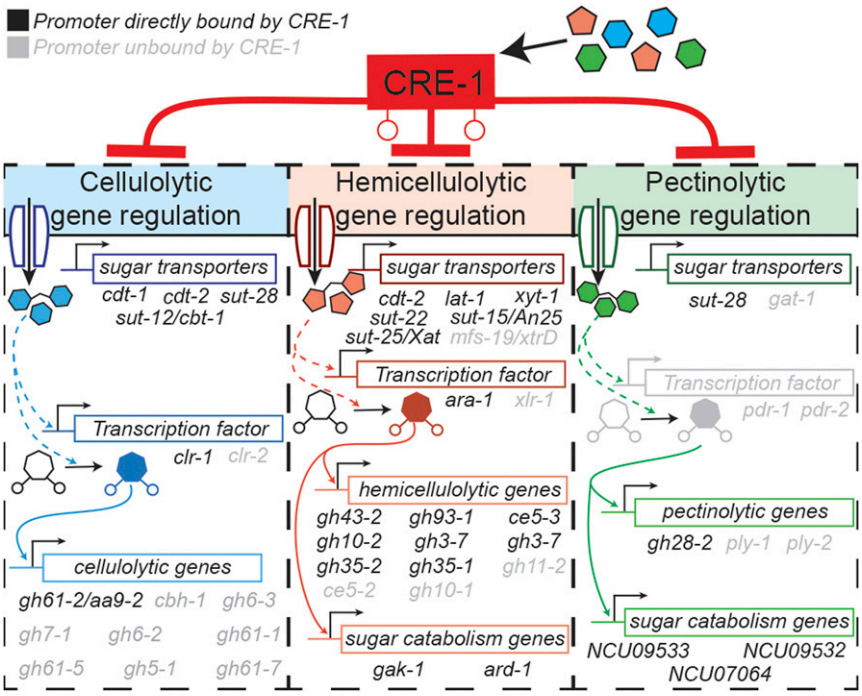

Fig. 5. CRE-1–mediated carbon catabolite repression acts through sugar transporter, transcription factor, sugar catabolism, and PCWDE genes to regulate plant cell wall degradation. CRE-1 regulates expression of PCWDE regulons by repressing expression of sugar transporters, transcription factors, and genes involved in the utilization of plant biomass components. Sugars transported into the cell may play either a direct or indirect role in the activation of transcription factors necessary for cellulolytic, hemicellulolytic, and pectinolytic gene expression. The promoters of genes in black are directly bound by CRE-1, and the promoters of genes in gray are not bound by CRE-1. The blue, orange, and green arrows indicate regulation that occurs downstream of CRE-1–mediated repression.

xylanases (NCU02855, NCU04997), feruloyl esterase B (NCU09491), and acetyl xylan esterases (NCU08785, NCU04494) (Fig. 6*C*). Additional genes encoding PCWDEs that were down-regulated in the Δ*vib-1* mutant but did not have VIB-1 binding sites in their promoters, could be explained by reduced expression of *clr-2* or *pdr-2* (Fig. 6*C*), consistent with the severe growth defect on cellulose and pectin substrates in the Δ*vib-1* mutant.

Our DAP-seq data suggest that VIB-1 acts through *clr-2* to promote cellulase gene expression. However, ChIP-seq identified *vib-1* as a target of the cellulase regulator, CLR-1 (10). CLR-1 also binds to the promoter and is required for the expression of *clr-2* (10). These observations suggest an interplay in the regulation of *clr-2* by CLR-1 and VIB-1. To investigate these interactions, we measured cellulase production in a Δ*vib-1* Δ*clr-3* strain, where repression of CLR-1 activation in the absence of cellulose is relieved (48), and in a Δ*vib-1* Δ*cre-1* mutant, which eliminates regulation of *clr-1* by CRE-1. Both double-mutant strains showed higher cellulase activity than Δ*vib-1* cells (P-adj < 0.01), indicating that when relieved from either CLR-3– or CRE-1–mediated repression, CLR-1 was capable of activating cellulolytic gene expression in the absence of VIB-1 (*SI Appendix*, Fig. S6*B*). However, the cellulase activity of Δ*vib-1* Δ*clr-3* or Δ*vib-1* Δ*cre-1* cells was not as high as WT cells, indicating that CLR-1 and VIB-1 were both required for full activation of cellulase genes in *N. crassa* (P-adj < 0.01) (*SI Appendix*, Fig. S6*B*).

In addition to defects in growth on cellulose and pectin, *N. crassa* and *A. nidulans vib-1*/*xprG* mutants show reduced growth when BSA is the sole carbon or nitrogen source (44, 49). However, analyses of the VIB-1 regulon on BSA did not reveal a clear reason for this growth deficit. The expression of only three genes encoding predicted proteases/peptidases was significantly reduced in the Δ*vib-1* mutant compared to wild-type cells, including a metalloprotease (*mpr-8*; NCU07200), a carboxypeptidase (*mpr-14*; NCU07536), and a proteinase T (*spr-7*; NCU07159). An additional set of vitamin B6 synthesis genes also showed decreased expression in the Δ*vib-1* mutant specifically on BSA, including *pdx-1* (NCU06550) and *pdx-2* (NCU06549) that encode proteins that form the enzyme complex pyridoxal 5′-phosphate synthase or vitamin B6 synthase (Dataset S7). Pyridoxal 5′-phosphate is a cofactor for many enzymes involved in amino acid metabolism and other protein metabolic processes (50).

Discussion

In nature, the primary source of nutrients for *N. crassa* is plant biomass. In this study, we determined expression patterns of the laboratory strain of *N. crassa* during exposure to different types of carbon sources, including monosaccharides, disaccharides, oligosaccharides, and plant biomass. These results showed that *N. crassa* responds specifically to the constituents of plant biomass in a largely specific manner (e.g., genes encoding cellulases were induced upon exposure of *N. crassa* to cellobiose) but also revealed cross-regulation of genes encoding enzymes not found in the substrate (e.g., genes encoding some xylanases were induced upon exposure of *N. crassa* to cellobiose). Induction of PCWDEs by constituents of the plant cell wall, particularly cellobiose and xylose, have also been shown for other basidiomycete and ascomycete fungi (51–53). These data indicate that filamentous fungi respond specifically to the presence of the individual nutrient sources available but also that the cells anticipate the presence of additional nutrient sources. This anticipation is likely due to the fact that individual components of the plant cell wall are unlikely to be found alone in nature, and therefore expression profiles of fungi deconstructing plant biomass are shaped by the structure and composition of the plant cell wall.

Analyses of a large dataset of microarray transcriptomics data of *A. niger* exposed to different conditions and performed by multiple laboratories were used to generate coexpression networks (54). Here, WGCNA on *N. crassa* datasets from exposure

to different carbon sources under carefully controlled conditions identified 28 clusters of coregulated genes (Dataset S2). We were particularly interested in defining new transcription factors and regulons associated with plant biomass deconstruction and identified 34 transcription factors whose expression level varied across our panel. Of these, two transcription factor mutants, Δ*ara-1* and Δ*pdr-2*, showed a significantly different response to *Miscanthus* and pectin, respectively, compared to WT cells (Fig. 2) and a deficiency in the utilization of arabinose/galactose (Δ*ara-1*) and galacturonic acid and pectin (Δ*pdr-2*). Our transcriptional analyses showed that the expression of the *lat-1* transporter gene and the *ard-1* gene were significantly down-regulated in the Δ*ara-1* mutant. Loss of LAT-1 prevents arabinose transport (28), while *ard-1* encodes L-arabinitol-4-dehydrogenase, which catalyzes the second reaction of arabinose catabolism (55) as well as the third step of the oxidoreductive galactose catabolism (56). PDR-2 is involved in the regulation of genes encoding homogalacturonan backbone-degrading enzymes and galacturonic acid catabolic enzymes, similar to GaaR in *A. niger* and *B. cinerea* (13, 14). Activation of a number of pectinase genes, such as the endo-PGase *gh28-1*, were dependent on the presence of both PDR-1 and PDR-2 (Fig. 2 *B* and *D*). Further characterization of transcription factors associated with plant biomass deconstruction, including those identified in this study, will lead to a better understanding of metabolic cross talk and reveal direct and/or indirect influence on each other in a synergistic regulatory network important for temporal and spatial deconstruction of plant biomass.

To define the direct regulons of transcription factors involved in plant biomass deconstruction, we utilized DAP-seq, developed to assess the direct targets of predicted transcription factors in *Arabidopsis thaliana* (30). Unlike other methods of identifying DNA binding sites, DAP-seq has the advantage that chromatin structure and growth conditions do not play a role in determining transcription factor binding sites. However, transcription factors that require chromatin structure or other cofactors to bind to their DNA target site will not be identified by DAP-seq. Our comparison of ChIP-seq and DAP-seq data for CLR-2 and XLR-1 showed a strong overlap in these two datasets. Analyses of both datasets were helped substantially by the availability of RNA-seq data of the deletion mutants exposed to relevant carbon sources. Although we identified 34 transcription factors whose expression varied across our transcriptional profiling dataset, mutants in a majority of these transcription factors did not show an obvious expression profile difference compared to WT when shifted to conditions where their expression increased (Dataset S1). This result could be due to redundancy of transcription factor function in nutrient regulation, a role of the transcription factor at a different time point than what was assessed in this study, or a role in cross-regulation that was not obvious from the RNA-seq dataset. We predict that these transcription factors do play a role in nutrient regulation in *N. crassa* and that a combination of DAP-seq to help identify conditions and timing for RNA-seq and expression profiling may help to illuminate their function. We may also have missed direct targets of transcription factors using either DAP-seq/RNA-seq or ChIP-seq/RNA-seq methods due to our stringent differential expression requirements (at least $2^{1.5}$-fold) from expression analyses taken at a single time point.

Our DAP-seq data indicated that CRE-1–mediated carbon catabolite repression acts not only through regulation of PCWDEs and their positive transcription factor regulators, but also through key sugar catabolic genes and sugar transporters. Repression of transporter gene expression by CRE-1 may reduce entry of signal-transducing sugars into the cell, thus limiting induction of genes encoding PCWDEs. In *A. niger*, low concentrations of galacturonic acid were required to induce gene expression of galacturonic acid utilization genes, including a galacturonic acid transporter, which was repressed by glucose in a CreA-dependent manner (57). Thus, CRE-1 may be regulating carbon catabolite repression through more than four levels of control or a "quadruple-lock" mechanism: 1) regulating expression of

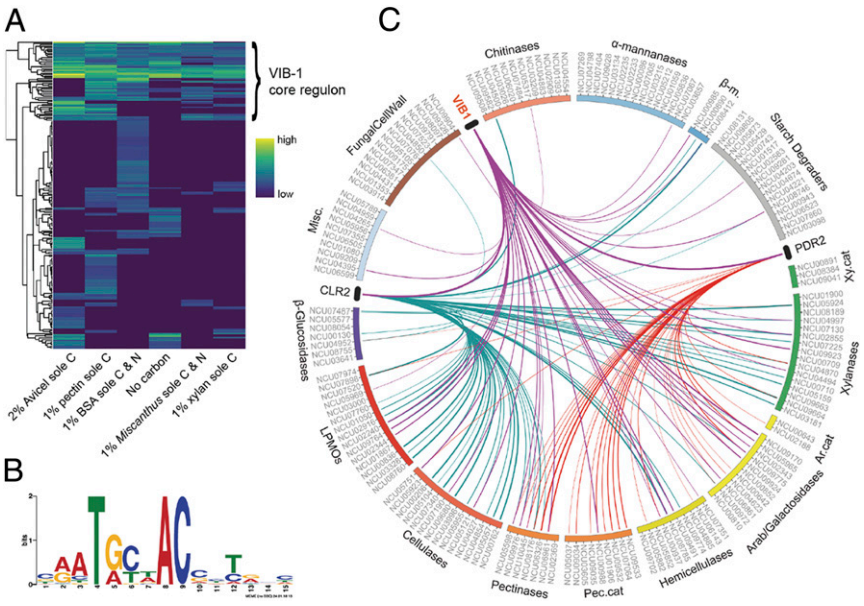

Fig. 6. VIB-1 regulon. (*A*) Hierarchical clustering of $\log_2$ fold change values from differential expression analysis of FGSC2489 versus Δ*vib-1* strains shifted to the indicated carbon conditions. Only genes with greater than $2^{1.5}$-fold change in at least one of the indicated conditions and with promoters bound by VIB-1 via DAP-seq are included. The VIB-1 core regulon is a cluster of genes that were differentially expressed across multiple conditions (Dataset S7). (*B*) VIB-1 binding motif built using MEME v4.12.0 using DAP binding peak sequences of VIB-1 core regulon. *E* value = 1.8^{-89}. (*C*) Plot built with Circos, version 0.69 (80), to display positive regulation of a catabolic CAZymes by VIB-1 and the transcription factors CLR-1 and PDR-2, which are bound and directly regulated by VIB-1. The thickness of the line corresponds to degree of fold change between WT and transcription factor mutant (Datasets S4 and S7), with thicker lines indicating a higher fold change.

sugar transporters; 2) regulating expression of sugar catabolic genes; 3) regulating expression of transcription factors important for expression of genes encoding PCWDEs; and 4) regulating the expression of genes encoding PCWDEs (Fig. 5). This quadruple-lock mechanism may be important in nutrient sensing, in production of specific PCWDEs based on nutrient source, and for integration of different nutrient signals for optimal metabolic regulation during plant biomass deconstruction. Our DAP-seq data on CRE-1 provide a framework for investigating the variety of conditions where CRE-1 plays a role in regulating metabolism (Dataset S6), particularly in conjunction with transcription factors that control condition-specific responses.

The transcription factor VIB-1 belongs to the p53 superfamily, which in mammalian cells regulates the cell cycle, DNA repair, and apoptosis (58). In *Saccharomyces cerevisiae*, the p53 homolog, Ndt80, regulates entry into meiosis upon nitrogen starvation (59). The genome of *N. crassa* has three p53 homologs, *vib-1*, *fsd-1*, and NCU04729, none of which is required for meiosis, although both *fsd-1* and *vib-1* mutants affect female reproductive structure development, which is regulated by nutritional status (60). In filamentous fungi, *vib-1* homologs have been shown to regulate protease production, production of extracellular hydrolases and PCWDEs, *N*-acetyl glucosamine catabolism, and secondary metabolism (61). Additionally, a *vib-1* homolog in the human pathogen *Candida albicans* regulates virulence (62). These observations suggest a general role for VIB-1 orthologs in sensing and responding to the availability of nutrients in their environment. In *N. crassa*, upon starvation, VIB-1 is required for an increase in the expression of a number of secreted proteins associated with polysaccharide and protein degradation (VIB-1 core regulon). These "scout" enzymes release mono/di/oligosaccharides from the insoluble carbohydrates in the plant cell wall, which are transported into the cell, resulting in the full activation of genes and secretion of enzymes associated with the utilization of a particular plant biomass component. This model is consistent with VIB-1 functioning as a general starvation response transcription factor, or a transcription factor important for basal expression of nutrient acquisition genes. In cells lacking VIB-1, this positive-feedback loop is not fully initiated, and full expression of the PCWDE genes necessary for optimal utilization of plant biomass is not achieved. Also consistent with this model, is that *vib-1* is not under carbon catabolite repression regulation, as the VIB-1 promoter is not bound by CRE-1 and limited overlap was observed between the VIB-1 regulon and CRE-1 binding sites (13 of 239 genes in VIB-1 regulon).

Previously, it was hypothesized that VIB-1 functions upstream of CRE-1 and COL-26, as the introduction of Δ*cre-1* Δ*col-26* mutations into a Δ*vib-1* mutant suppressed the inability of the Δ*vib-1* mutant to utilize cellulose (21). Our DAP-seq and RNA-seq data support an alternative hypothesis. We predict that the deletion of *cre-1* and *col-26* allows sufficient expression of *clr-2*, and, thus, downstream enzymes and transporters necessary for cellulose degradation, to restore growth of the *Δvib-1* mutant on cellulose (partly due to a lack of repression of the cellodextrin transporters by CRE-1) in a manner similar to how deletion of the three β-glucosidase genes restored cellulase production in the *Δvib-1* mutant on cellobiose (48). Under carbon-limiting conditions, VIB-1 promotes expression of *clr-2* and *pdr-2* along with a small set of PCWDEs. These secreted enzymes cleave plant biomass and signaling sugars are transported into the cell. For cellulose utilization, cellobiose (or a modified version of cellobiose) results in inactivation of the repressor CLR-3 (48), allowing activation of CLR-1. CLR-1 promotes expression of *clr-2* and cellulases and, together with VIB-1, results in full expression of *clr-2* and induction of a positive-feedback loop. As the glucose concentration increases inside the cell, CRE-1–mediated carbon catabolite repression is activated, reducing expression of *clr-1* and cellodextrin transporters *cdt-1*, *cdt-2*, and *cbt-1*, thus negatively regulating expression of PCWDEs both by limiting the expression of *clr-1* and the cleaving and import of sugar signaling molecules (Fig. 5). Our data support the cooperative regulation of PCWDEs by negative regulation of transporters by CRE-1 and positive regulation of enzyme scouts that regulate signaling processes via VIB-1.

VIB-1 regulation of HET domain genes may also play a role in nutrient acquisition. HET domain genes allow fungi to distinguish between self and nonself, and initiate programmed cell death upon fusion between nonself colonies (63). Starvation increases vegetative cell fusion frequency in a number of ascomycete fungi, including *N. crassa* (64–66). We hypothesize that VIB-1 increases expression of these HET domain genes to ensure viable fusion is prevented between nonself cells. Potentially, this activity may also be related to the regulation of secondary metabolism by VIB-1-like proteins. The promoters of LaeA-like methyltransferase domain-containing proteins were abundant in the direct target gene set of VIB-1. LaeA and LaeA-like methyltransferase orthologs are negative regulators of secondary metabolite production in fungi (47, 67, 68). The modulation of the expression of these methyltransferases by VIB-1 may have downstream gene-regulatory consequences that may affect competition among microbes and nutrient acquisition during plant biomass deconstruction and utilization.

Materials and Methods

Comprehensive List of PCWDE Genes in the *N. crassa* Genome. A comprehensive list of predicted *N. crassa* genes encoding PCWDE was compiled by examining all CAZymes from the Carbohydrate Active Enzymes Database (http://www.cazy.org) (69) (*SI Appendix*, Table S2).

Strains, Growth Conditions, RNA Extraction, and RNA-Seq. Strains are listed in *SI Appendix*, Table S3 (see *SI Appendix, Supplemental Materials and Methods* for strain construction). For RNA-seq experiments induction conditions, 2 mM monosaccharides and disaccharides were used (23); for complex polysaccharides and plant biomass, 1% (wt/vol) was used (*SI Appendix*, Table S1). RNA isolation and RNA-seq methods are described in *SI Appendix, Supplemental Materials and Methods*. Filtered reads were mapped against the *N. crassa* OR74A genome (v12) using Tophat 2.0.4 (70) and transcript abundance was estimated with Cufflinks 2.0.2 (71) in fragments per kilobase of transcript per million mapped reads (FPKMs) using upper quartile normalization. Differential expression analysis was performed on raw counts with DEseq2, version 3.3 (72), using data from biological triplicates.

WGCNA and FUNCAT Analyses. The gene coexpression network was calculated across expression profiles for the WT strain exposed to carbon sources listed in Dataset S1 using the R package WGCNA (26) and a custom catalog (11) based on MPS Functional Catalogue Database (FuncatDB) (73) with expanded categories for cell wall degradation-related genes for enrichment analysis.

Enzyme Activity and Transport Assays. WT and Δ*cre-1* strains were induced in 0.5% pectin or 0.5% pectin plus 2% D-glucose and transferred to either 100 μM L-rhamnose or 100 μM L-rhamnose plus 100 μM D-glucose as uptake solution. WT and Δ*sut-28* strains were transferred to uptake solutions containing either 100 μM L-rhamnose, 90 μM D-fucose (VWR; A16789), 90 μM D-xylose, or 90 μM D-galactose (Sigma-Aldrich; G0750). Monosaccharide concentration of sample supernatants was quantified by high pH anion exchange chromatography–pulsed amperometric detection on an ICS-3000 instrument (Thermo Scientific). A 25-μL sample was injected onto a Dionex CarboPac PA20 column (3 × 30-mm guard and 3 × 150-mm analytical) and eluted using an isocratic mobile phase of 10 mM NaOH at 0.4 mL/min and 30 °C over 12 min. Cellulase activity assays were modified from Coradetti et al. (27) (*SI Appendix, Supplemental Materials and Methods*).

DAP-Seq. Predicted open reading frames for each transcription factor were amplified from cDNA generated using RNA to cDNA EcoDry premix (Clontech). Amplified transcription factor sequences were inserted into an expression vector containing T7 and SP6 promoters upstream of HALO tag as previously described (30). In vitro transcription and translation of transcription factors was performed using Promega TnT T7 Rabbit Reticulocyte Quick Coupled Transcription/Translation System by incubating 1 μg of plasmid DNA with 60 μL of TnT Master Mix and 1.5 μL of 1 mM methionine overnight at room temperature. Expression was verified using Western blot analysis with Promega

Anti-HaloTag monoclonal antibody. Single DAP-seq libraries were generated once for each transcription factor, tested, and sequenced once with Illumina MiSeq 2 × 150-bp runs.

Filtered reads were aligned to the *N. crassa* OR74A genome (v12) using Bowtie2 v2.3.2 (70). Peak calling was performed using MACS2 v2.1.1 (74) with *P* value cutoff at 0.001 and utilizing negative control library alignments. Peaks within 3,000 bp upstream of translation start sites were selected for and annotated using a custom Python script. The same Python script was used for reanalysis of ChIP-seq peaks dataset from Craig et al. (10) for DAP-seq/ChIP-seq comparisons.

Data Availability. The RNA-seq data reported in this paper have been deposited in the Joint Genome Institute Genome Portal (75), in the National Center for Biotechnology Information (NCBI) Sequence Read Archive (ID SRP133337), and in the NCBI BioProject database (76). Data are also provided for processed RNA-seq experiments in Datasets S1, S4, S5, and S7 (75–78). DAP-seq data reported in this paper have been deposited in the NCBI Sequence Read Archive (ID SRP133627). Standard Neurospora methods information is available from the Fungal Genetics Stock Center (FGSC) at http://www.fgsc.net/Neurospora/NeurosporaProtocolGuide.htm. A list of *N. crassa* deletion strains and strains constructed for this study are available in *SI Appendix*, Table S3. Strains in this table are available from the FGSC (http://www.fgsc.net/ncrassa.html).

ACKNOWLEDGMENTS. We acknowledge the use of deletion strains generated by Grant P01 GM-068087 "Functional Analysis of a Model Filamentous Fungus" and that are publicly available at the Fungal Genetics Stock Center. This work was supported by an Energy Biosciences Institute Grant, a Laboratory Directed Research and Development Program of Lawrence Berkeley National Laboratory under US Department of Energy Contract DE-AC02-05CH11231, a Joint Genome Institute Community Science Program grant (CSP 982), and funds from the Fred E. Dickinson Chair of Wood Science and Technology to N.L.G. V.W.W. was partially supported by National Institutes of Health National Research Service Award Trainee Grant 5T32GM007127-39. The work conducted by the US Department of Energy (DOE) Joint Genome Institute, a DOE Office of Science User Facility, was supported by the Office of Science of the US DOE under Contract no. DE-AC02-05CH11231. We thank Elias Bleek (Technical University of Munich) for assistance with transporter assays and Jamie Irvine, Jimmy Schmidt, and Kyler Murlas for expected value calculations from CRE-1 DAP-seq and microarray datasets.

1. C. W. Fernandez, P. G. Kennedy, Revisiting the "Gadgil effect": Do interguild fungal interactions control carbon cycling in forest soils? *New Phytol.* **209**, 1382–1394 (2016).
2. V. K. Gupta *et al.*, Fungal enzymes for bio-products from sustainable and waste biomass. *Trends Biochem. Sci.* **41**, 633–645 (2016).
3. K. H. Caffall, D. Mohnen, The structure, function, and biosynthesis of plant cell wall pectic polysaccharides. *Carbohydr. Res.* **344**, 1879–1900 (2009).
4. A. J. Ragauskas *et al.*, Lignin valorization: Improving lignin processing in the biorefinery. *Science* **344**, 1246843 (2014).
5. E. Kunitake, T. Kobayashi, Conservation and diversity of the regulators of cellulolytic enzyme genes in Ascomycete fungi. *Curr. Genet.* **63**, 951–958 (2017).
6. L. B. Huberman, J. Liu, L. Qin, N. L. Glass, Regulation of the lignocellulolytic response in filamentous fungi. *Fungal Biol. Rev.* **30**, 101–111 (2016).
7. T. Furukawa *et al.*, Identification of specific binding sites for XYR1, a transcriptional activator of cellulolytic and xylanolytic genes in *Trichoderma reesei*. *Fungal Genet. Biol.* **46**, 564–574 (2009).
8. A. A. Hasper, L. M. Trindade, D. van der Veen, A. J. J. van Ooyen, L. H. de Graaff, Functional analysis of the transcriptional activator XlnR from *Aspergillus niger*. *Microbiology* **150**, 1367–1375 (2004).
9. K. Brunner, A. M. Lichtenauer, K. Kratochwill, M. Delic, R. L. Mach, Xyr1 regulates xylanase but not cellulase formation in the head blight fungus *Fusarium graminearum*. *Curr. Genet.* **52**, 213–220 (2007).
10. J. P. Craig, S. T. Coradetti, T. L. Starr, N. L. Glass, Direct target network of the *Neurospora crassa* plant cell wall deconstruction regulators CLR-1, CLR-2, and XLR-1. *MBio* **6**, e01452-15 (2015).
11. N. Thieme *et al.*, The transcription factor PDR-1 is a multi-functional regulator and key component of pectin deconstruction and catabolism in *Neurospora crassa*. *Biotechnol. Biofuels* **10**, 149 (2017).
12. B. S. Gruben *et al.*, *Aspergillus niger* RhaR, a regulator involved in L-rhamnose release and catabolism. *Appl. Microbiol. Biotechnol.* **98**, 5531–5540 (2014).
13. E. Alazi *et al.*, The transcriptional activator GaaR of *Aspergillus niger* is required for release and utilization of D-galacturonic acid from pectin. *FEBS Lett.* **590**, 1804–1815 (2016).
14. L. Zhang *et al.*, A novel Zn2 Cys6 transcription factor BcGaaR regulates D-galacturonic acid utilization in *Botrytis cinerea*. *Mol. Microbiol.* **100**, 247–262 (2016).
15. E. Battaglia *et al.*, Analysis of regulation of pentose utilisation in *Aspergillus niger* reveals evolutionary adaptations in Eurotiales. *Stud. Mycol.* **69**, 31–38 (2011).
16. S. Klaubauf, M. Zhou, M. H. Lebrun, R. P. de Vries, E. Battaglia, A novel L-arabinose-responsive regulator discovered in the rice-blast fungus *Pyricularia oryzae* (*Magnaporthe oryzae*). *FEBS Lett.* **590**, 550–558 (2016).
17. J. Sun, N. L. Glass, Identification of the CRE-1 cellulolytic regulon in *Neurospora crassa*. *PLoS One* **6**, e25654 (2011).
18. L. N. Ries, S. R. Beattie, E. A. Espeso, R. A. Cramer, G. H. Goldman, Diverse regulation of the CreA carbon catabolite repressor in *Aspergillus nidulans*. *Genetics* **203**, 335–352 (2016).
19. Y. Xiong *et al.*, A fungal transcription factor essential for starch degradation affects integration of carbon and nitrogen metabolism. *PLoS Genet.* **13**, e1006737 (2017).
20. M. Nitta *et al.*, A new $Zn(II)_2Cys_6$-type transcription factor BglR regulates β-*glucosidase* expression in *Trichoderma reesei*. *Fungal Genet. Biol.* **49**, 388–397 (2012).
21. Y. Xiong, J. Sun, N. L. Glass, VIB1, a link between glucose signaling and carbon catabolite repression, is essential for plant cell wall degradation by *Neurospora crassa*. *PLoS Genet.* **10**, e1004500 (2014).
22. C. Ivanova *et al.*, Genome sequencing and transcriptome analysis of *Trichoderma reesei* QM9978 strain reveals a distal chromosome translocation to be responsible for loss of *vib1* expression and loss of cellulase induction. *Biotechnol. Biofuels* **10**, 209 (2017).
23. E. A. Znameroski *et al.*, Induction of lignocellulose-degrading enzymes in *Neurospora crassa* by cellodextrins. *Proc. Natl. Acad. Sci. U.S.A.* **109**, 6012–6017 (2012).
24. M. M. Gielkens, E. Dekkers, J. Visser, L. H. de Graaff, Two cellobiohydrolase-encoding genes from *Aspergillus niger* require D-xylose and the xylanolytic transcriptional activator XlnR for their expression. *Appl. Environ. Microbiol.* **65**, 4340–4345 (1999).
25. M. H. Saier, Jr *et al.*, The Transporter Classification Database (TCDB): Recent advances. *Nucleic Acids Res.* **44**, D372–D379 (2016).
26. P. Langfelder, S. Horvath, WGCNA: An R package for weighted correlation network analysis. *BMC Bioinformatics* **9**, 559 (2008).
27. S. T. Coradetti *et al.*, Conserved and essential transcription factors for cellulase gene expression in ascomycete fungi. *Proc. Natl. Acad. Sci. U.S.A.* **109**, 7397–7402 (2012).
28. J. P. Benz *et al.*, A comparative systems analysis of polysaccharide-elicited responses in *Neurospora crassa* reveals carbon source-specific cellular adaptations. *Mol. Microbiol.* **91**, 275–299 (2014).
29. T. Benocci *et al.*, ARA1 regulates not only l-arabinose but also D-galactose catabolism in *Trichoderma reesei*. *FEBS Lett.* **592**, 60–70 (2018).
30. R. C. O'Malley *et al.*, Cistrome and epicistrome features shape the regulatory DNA landscape. *Cell* **165**, 1280–1292 (2016).
31. C. Derntl *et al.*, Mutation of the Xylanase regulator 1 causes a glucose blind hydrolase expressing phenotype in industrially used *Trichoderma* strains. *Biotechnol. Biofuels* **6**, 62 (2013).
32. M. Adnan *et al.*, Carbon catabolite repression in filamentous fungi. *Int. J. Mol. Sci.* **19**, E48 (2017).
33. E. A. Espeso, M. A. Peñalva, In vitro binding of the two-finger repressor CreA to several consensus and non-consensus sites at the ipnA upstream region is context dependent. *FEBS Lett.* **342**, 43–48 (1994).
34. E. N. Tamayo *et al.*, CreA mediates repression of the regulatory gene *xlnR* which controls the production of xylanolytic enzymes in *Aspergillus nidulans*. *Fungal Genet. Biol.* **45**, 984–993 (2008).
35. B. Wang *et al.*, Identification and characterization of the glucose dual-affinity transport system in *Neurospora crassa*: Pleiotropic roles in nutrient transport, signaling, and carbon catabolite repression. *Biotechnol. Biofuels* **10**, 17 (2017).
36. J. Sloothaak, D. I. Odoni, V. A. Martins Dos Santos, P. J. Schaap, J. A. Tamayo-Ramos, Identification of a novel L-rhamnose uptake transporter in the filamentous fungus *Aspergillus niger*. *PLoS Genet.* **12**, e1006468 (2016).
37. J. M. Galazka *et al.*, Cellodextrin transport in yeast for improved biofuel production. *Science* **330**, 84–86 (2010).
38. Y. Xiong *et al.*, The proteome and phosphoproteome of *Neurospora crassa* in response to cellulose, sucrose and carbon starvation. *Fungal Genet. Biol.* **72**, 21–33 (2014).
39. X. Li *et al.*, Cellobionic acid utilization: From *Neurospora crassa* to *Saccharomyces cerevisiae*. *Biotechnol. Biofuels* **8**, 120 (2015).
40. X. Li *et al.*, Expanding xylose metabolism in yeast for plant cell wall conversion to biofuels. *eLife* **4**, e05896 (2015).
41. E. A. Znameroski *et al.*, Evidence for transceptor function of cellodextrin transporters in *Neurospora crassa*. *J. Biol. Chem.* **289**, 2610–2619 (2014).
42. J. Du, S. Li, H. Zhao, Discovery and characterization of novel D-xylose-specific transporters from *Neurospora crassa* and *Pichia stipitis*. *Mol. Biosyst.* **6**, 2150–2156 (2010).
43. J. Li, L. Lin, H. Li, C. Tian, Y. Ma, Transcriptional comparison of the filamentous fungus *Neurospora crassa* growing on three major monosaccharides D-glucose, D-xylose and L-arabinose. *Biotechnol. Biofuels* **7**, 31 (2014).
44. K. Dementhon, G. Iyer, N. L. Glass, VIB-1 is required for expression of genes necessary for programmed cell death in *Neurospora crassa*. *Eukaryot. Cell* **5**, 2161–2173 (2006).
45. Q. Xiang, N. L. Glass, Identification of *vib-1*, a locus involved in vegetative incompatibility mediated by *het-c* in *Neurospora crassa*. *Genetics* **162**, 89–101 (2002).
46. J. Zhao *et al.*, Identification of allorecognition loci in *Neurospora crassa* by genomics and evolutionary approaches. *Mol. Biol. Evol.* **32**, 2417–2432 (2015).
47. J. W. Bok, N. P. Keller, LaeA, a regulator of secondary metabolism in *Aspergillus* spp. *Eukaryot. Cell* **3**, 527–535 (2004).
48. L. B. Huberman, S. T. Coradetti, N. L. Glass, Network of nutrient-sensing pathways and a conserved kinase cascade integrate osmolarity and carbon sensing in *Neurospora crassa*. *Proc. Natl. Acad. Sci. U.S.A.* **114**, E8665–E8674 (2017).
49. M. E. Katz, K.-A. Gray, B. F. Cheetham, The *Aspergillus nidulans xprG* (*phoG*) gene encodes a putative transcriptional activator involved in the response to nutrient limitation. *Fungal Genet. Biol.* **43**, 190–199 (2006).

50. G. Mittenhuber, Phylogenetic analyses and comparative genomics of vitamin B6 (pyridoxine) and pyridoxal phosphate biosynthesis pathways. *J. Mol. Microbiol. Biotechnol.* **3**, 1–20 (2001).
51. S. Casado López *et al*., Induction of genes encoding plant cell wall-degrading carbohydrate-active enzymes by lignocellulose-derived monosaccharides and cellobiose in the white-rot rungus *Dichomitus squalens*. *Appl. Environ. Microbiol.* **84**, e00403-18 (2018).
52. W. Zhang *et al*., Two major facilitator superfamily sugar transporters from *Trichoderma reesei* and their roles in induction of cellulase biosynthesis. *J. Biol. Chem.* **288**, 32861–32872 (2013).
53. M. Brienzo, J. R. Monte, A. M. Milagres, Induction of cellulase and hemicellulase activities of *Thermoascus aurantiacus* by xylan hydrolyzed products. *World J. Microbiol. Biotechnol.* **28**, 113–119 (2012).
54. P. Schäpe *et al*., Updating genome annotation for the microbial cell factory *Aspergillus niger* using gene co-expression networks. *Nucleic Acids Res.* **47**, 559–569 (2019).
55. B. Seiboth, B. Metz, Fungal arabinan and L-arabinose metabolism. *Appl. Microbiol. Biotechnol.* **89**, 1665–1673 (2011).
56. D. Mojzita, S. Herold, B. Metz, B. Seiboth, P. Richard, L-Xylo-3-hexulose reductase is the missing link in the oxidoreductive pathway for D-galactose catabolism in filamentous fungi. *J. Biol. Chem.* **287**, 26010–26018 (2012).
57. J. Niu *et al*., The interaction of induction and repression mechanisms in the regulation of galacturonic acid-induced genes in *Aspergillus niger*. *Fungal Genet. Biol.* **82**, 32–42 (2015).
58. S. Haupt, I. Louria-Hayon, Y. Haupt, P53 licensed to kill? Operating the assassin. *J. Cell. Biochem.* **88**, 76–82 (2003).
59. L. Xu, M. Ajimura, R. Padmore, C. Klein, N. Kleckner, NDT80, a meiosis-specific gene required for exit from pachytene in *Saccharomyces cerevisiae*. *Mol. Cell. Biol.* **15**, 6572–6581 (1995).
60. E. A. Hutchison, N. L. Glass, Meiotic regulators Ndt80 and ime2 have different roles in *Saccharomyces* and *Neurospora*. *Genetics* **185**, 1271–1282 (2010).
61. M. E. Katz, Nutrient sensing—the key to fungal p53-like transcription factors? *Fungal Genet. Biol.* **124**, 8–16 (2019).
62. K. Min, A. Biermann, D. A. Hogan, J. B. Konopka, Genetic analysis of NDT80 family transcription factors in *Candida albicans* using new CRISPR-Cas9 approaches. *MSphere* **3**, e00545-18 (2018).
63. A. Daskalov, J. Heller, S. Herzog, A. Fleißner, N. L. Glass, Molecular mechanisms regulating cell fusion and heterokaryon formation in filamentous fungi. *Microbiol. Spectr.*, 10.1128/microbiolspec.FUNK-0015-2016 (2017).
64. M. G. Roca, M. Weichert, U. Siegmund, P. Tudzynski, A. Fleissner, Germling fusion via conidial anastomosis tubes in the grey mould *Botrytis cinerea* requires NADPH oxidase activity. *Fungal Biol.* **116**, 379–387 (2012).
65. F. H. Ishikawa, E. A. Souza, N. D. Read, M. G. Roca, Live-cell imaging of conidial fusion in the bean pathogen, *Colletotrichum lindemuthianum*. *Fungal Biol.* **114**, 2–9 (2010).
66. V. Fischer-Harman, K. J. Jackson, A. Muñoz, J. Y. Shoji, N. D. Read, Evidence for tryptophan being a signal molecule that inhibits conidial anastomosis tube fusion during colony initiation in *Neurospora crassa*. *Fungal Genet. Biol.* **49**, 896–902 (2012).
67. Q. Bi, D. Wu, X. Zhu, B. Gillian Turgeon, *Cochliobolus heterostrophus Llm1*—a Lae1-like methyltransferase regulates T-toxin production, virulence, and development. *Fungal Genet. Biol.* **51**, 21–33 (2013).
68. J. M. Palmer *et al*., Secondary metabolism and development is mediated by LlmF control of VeA subcellular localization in *Aspergillus nidulans*. *PLoS Genet.* **9**, e1003193 (2013).
69. V. Lombard, H. Golaconda Ramulu, E. Drula, P. M. Coutinho, B. Henrissat, The carbohydrate-active enzymes database (CAZy) in 2013. *Nucleic Acids Res.* **42**, D490–D495 (2014).
70. D. Kim *et al*., TopHat2: Accurate alignment of transcriptomes in the presence of insertions, deletions and gene fusions. *Genome Biol.* **14**, R36 (2013).
71. C. Trapnell *et al*., Differential analysis of gene regulation at transcript resolution with RNA-seq. *Nat. Biotechnol.* **31**, 46–53 (2013).
72. M. I. Love, W. Huber, S. Anders, Moderated estimation of fold change and dispersion for RNA-seq data with DESeq2. *Genome Biol.* **15**, 550 (2014).
73. A. Ruepp *et al*., The FunCat, a functional annotation scheme for systematic classification of proteins from whole genomes. *Nucleic Acids Res.* **32**, 5539–5545 (2004).
74. Y. Zhang *et al*., Model-based analysis of ChIP-seq (MACS). *Genome Biol.* **9**, R137 (2008).
75. N. L. Glass, The Fungal Nutritional ENCODE project. JGI Genome Portal. https://genome.jgi.doe.gov/portal/TheFunENCproject/TheFunENCproject.info.html. Deposited 16 February 2016.
76. V. W. Wu, D. J. Kowbel, RNAseq for the regulatory and transcriptional landscape associated with carbon utilization in a filamentous fungus *Neurospora crassa* FGSC2489. NCBI BioProject. https://www.ncbi.nlm.nih.gov/bioproject/594366. Deposited 9 December 2019.
77. V. W. Wu, *Neurospora crassa* transcription factor DAPseq. NCBI Sequence Read Archive. https://www.ncbi.nlm.nih.gov/sra/SRP133627. Deposited 27 February 2018.
78. V. W. Wu, *Neurospora crassa* VIB-1 RNAseq. NCBI Sequence Read Archive. https://www.ncbi.nlm.nih.gov/sra/SRP133337. Deposited 23 February 2018.
79. P. Shannon *et al*., Cytoscape: A software environment for integrated models of biomolecular interaction networks. *Genome Res.* **13**, 2498–2504 (2003).
80. M. Krzywinski *et al*., Circos: An information aesthetic for comparative genomics. *Genome Res.* **19**, 1639–1645 (2009).